Sottrup-Jensen, L., Claeys, H., Zajdel, M., Peterson, T. E., & Magnusson, S. (1978) *Prog. Chem. Fibrinolysis Thrombolysis 3*, 191-209.
Suenson, E., & Thorsen, S. (1982) *Biochem. J. 197*, 619-628.
Suenson, E., & Thorsen, S. (1988) *Biochemistry 27*, 2435-2443.
Suenson, E., & Petersen, L. C. (1989) *Fibrinolysis 3*, 17.
Thorsen, S. (1975) *Biochim. Biophys. Acta 251*, 363-369.
Trexler, M., & Patthy, L. (1983) *Proc. Natl. Acad. Sci. U.S.A. 80*, 2457-2461.
Urano, T., Chibber, B. A. K., & Castellino, F. J. (1987a) *Proc. Natl. Acad. Sci. U.S.A. 84*, 4031-4034.
Urano, T., de Serrano, V. S., Chibber, B. A. K., & Castellino, F. J. (1987b) *J. Biol. Chem. 262*, 15959-15964.
Vali, Z., & Patthy, L. (1982) *J. Biol. Chem. 257*, 2104-2110.
Varadi, A., & Patthy, L. (1981) *Biochem. Biophys. Res. Commun. 103*, 97-102.
Varadi, A., & Patthy, L. (1983) *Biochemistry 22*, 2440-2446.
Violand, B. N., Bryne, R., & Castellino, F. J. (1978) *J. Biol. Chem. 253*, 5395-5401.
Wallen, P., & Wiman, B. (1972) *Biochim. Biophys. Acta 257*, 122-142.
Wallen, P., & Wiman, B. (1975) *Cold Spring Harbor Conf. Cell Proliferation 2*, 291-303.
Walther, P. J., Hill, R. L., & McKee, P. A. (1975) *J. Biol. Chem. 250*, 5926-5933.
Wiman, B., & Collen, D. (1978) *Nature (London) 272*, 549-550.

^{31}P ENDOR Studies of Xanthine Oxidase: Coupling of Phosphorus of the Pterin Cofactor to Molybdenum(V)†

Barry D. Howes,‡ Brian Bennett,‡ Alrik Koppenhöfer,‡ David J. Lowe,§ and Robert C. Bray*,‡
School of Chemistry and Molecular Sciences, University of Sussex, Brighton BN1 9QJ, U.K., and AFRC IPSR Nitrogen Fixation Laboratory, University of Sussex, Brighton BN1 9RQ, U.K.
Received July 13, 1990; Revised Manuscript Received January 9, 1991

ABSTRACT: ^{31}P ENDOR spectra are described for three different molybdenum(V) species in reduced xanthine oxidase samples. The spectra were not affected by removing the FAD from the enzyme, implying that this is located at some distance from molybdenum. Furthermore, in confirmation of the work of J. L. Johnson, R. E. London, and K. V. Rajagopalan [(1989) *Proc. Natl. Acad. Sci. U.S.A. 86*, 6493-6497], NMR and chemical analysis of the phosphate content of highly purified xanthine oxidase showed there are only three phosphate residues per subunit of the enzyme. It is concluded that the ENDOR features are due to hyperfine coupling of the phosphate group of the pterin cofactor to the molybdenum atom. Evaluation of the dipolar component of the coupling has permitted estimation of the molybdenum-phosphorus distances as 7-12 Å. This implies that the cofactor is in an extended conformation in the enzyme molecule. Less detailed ^{31}P ENDOR data on sulfite oxidase are consistent with a similar conformation for the cofactor in this enzyme.

The molybdenum enzymes are found in organisms from bacteria to man and display a variety of roles. They have been studied for many years by using a number of physical and biochemical techniques (Bray, 1988). There are, however, as yet no X-ray crystallographic data on the enzymes, and amino acid sequence information is only just beginning to contribute [cf. Wootton et al. (1991)]. Major contributions to our understanding of the mechanisms by which molybdenum enzymes function have been made by EPR spectroscopy of molybdenum(V). However, despite the extensive literature, structural information on the enzymes, even on the immediate environment of the metal, is still in need of expansion. This is partly because ligand hyperfine splittings from some nuclei may be too small to be resolved in EPR spectra. These atoms therefore remain undetected, and structural analysis from their couplings is not possible.

The improved resolution of electron nuclear double resonance (ENDOR)[1] spectroscopy, its capacity to distinguish different nuclear types and to provide interatomic distances [cf. Hughes et al. (1990)], offers an ideal tool to extend considerably the information available through EPR spectroscopy. An improved insight into the disposition of particular ligands and the general structure of the metal ion binding site should be forthcoming from such studies. In this report, attention is focused on the extraction, from frozen solution ENDOR spectra, of structural data on the phosphorus atoms near the molybdenum in milk xanthine oxidase, the most extensively studied of the molybdenum enzymes. The molybdenum center of xanthine oxidase, at the molybdenum(V) oxidation level, can exist in a considerable number of different and clearly defined states. Some of these are derived from the active enzyme and some from inactive species. Each species gives rise to a characteristic EPR signal, and signals are distinguished by names such as Rapid, Inhibited, and Desulfo Inhibited. Structural information is available for each of these species, derived largely from EPR work involving substitution with stable isotopes (Bray, 1988). In the present work, we have used ENDOR spectroscopy to study in detail coupling of ^{31}P nuclei to molybdenum(V) in several of these species. We employed xanthine oxidase both in its normal form and as the deflavoenzyme, from which FAD has been removed (Bray, 1975). Less comprehensive studies have also been made on chicken liver sulfite oxidase. Such data have not been readily obtainable by other physical techniques,

† This work was supported through a grant for a Linked Research Group from the Agricultural and Food Research Council and by a grant from the Wellcome Trust. EPR equipment was provided by a grant from the Science and Engineering Research Council.
‡ School of Chemistry and Molecular Sciences, University of Sussex.
§ AFRC IPSR Nitrogen Fixation Laboratory, University of Sussex.

[1] Abbreviation: ENDOR, electron nuclear double resonance.

0006-2960/91/0430-3969$02.50/0

though molybdenum–phosphate interactions in low molecular weight models for the pterin molybdenum cofactor are observable by NMR (Künsthardt & Enemark, 1987). We recently reported (Howes et al., 1990) on the proton ENDOR of xanthine oxidase, and extension of the work [cf. Howes et al. (1991)] to include studies of couplings of other ligands in the vicinity of molybdenum is clearly possible.

This work is the first detailed description of ^{31}P ENDOR from a metalloenzyme. The preliminary ^{31}P ENDOR studies of Pinhal et al. (1989) led us to seek to identify the phosphorus atom or atoms in the xanthine oxidase molecule that are coupled to molybdenum. The quest prompted us to reinvestigate the claim by Davis et al. (1984) that xanthine oxidase contains a phosphoserine residue, perhaps participating in catalysis. Our work on this topic, briefly reported here, has provided independent confirmation of the conclusion of Johnson et al. (1989) that the pure enzyme contains only 3 mol of phosphorus per half-molecule of enzyme, 1 mol in the pterin cofactor and 2 mol in the FAD. Our data make it clear that it is the phosphorus of the pterin cofactor that is coupled to the molybdenum and observed in the ENDOR spectra. They also provide important new information concerning the location of this phosphorus atom in relation to molybdenum in the enzymes. Preliminary reports on parts of the work have appeared (Bray et al., 1991; Pinhal et al., 1989).

Experimental Procedures

Enzymes. Milk xanthine oxidase was prepared by using selective denaturation with sodium salicylate [Hart et al., 1970; steps H1 and H2 of Ventom et al. (1988)]. An additional purification procedure consisting of affinity chromatography [Nishino et al., 1981; step N1 of Ventom et al. (1988)] followed by gel filtration on Sephacryl S-200 in 50 mM Na^+-Bicine buffer, pH 8.2, was employed for some samples. The enzyme was concentrated for ENDOR and for NMR by using Minicon B-15 concentrators (Amicon Ltd.). Concentrations of the enzyme half-molecule were estimated from measurements of the absorption at 450 nm with $\epsilon = 36\ mM^{-1}\ cm^{-1}$. The proportion of functional enzyme was estimated by assays with xanthine as substrate (Bray, 1975). Samples were stored as frozen beads at the temperature of liquid nitrogen. Freezing and thawing caused a small loss of FAD from the enzyme. This was readily detected during gel filtration by the separation of a flavin band with characteristic absorption maxima at 448 and 376 nm. The liberated flavin was estimated by taking $\epsilon(450\ nm) = 11.3\ mM^{-1}\ cm^{-1}$, and for some samples amounted to up to 4% of that originally present. The FAD loss was to some extent cumulative, amounting to about 15% in samples which had been frozen and thawed 10 times.

Desulfoxanthine oxidase was prepared by treating the enzyme with cyanide (Massey & Edmonson, 1970). The deflavo form was prepared by treating dithionite-reduced enzyme with KI (Kanda & Rajagopalan, 1972) and was found to have an A_{450}/A_{550} of 1.91, corresponding [cf. Komai et al. (1969)] to essentially complete flavin loss. The amount of material precipitating during the treatment was found to decrease markedly when 1 mM salicylate was employed throughout (Komai et al., 1969). Any precipitate present in the final product was removed by centrifugation at $20000g_{av}$, for 1 h at 4 °C.

Sulfite oxidase was partially purified from frozen chicken livers by a method similar to that of Kessler et al. (1974) and assayed as described by Lamy et al. (1980). It was found that, with careful fractionation with ammonium sulfate, the acetone fractionation, which required considerable care if serious loss of activity was to be avoided, could be omitted. The sample used for ENDOR had a specific activity of 25 μmol of cytochrome *c* reduced min^{-1} (mg of protein)$^{-1}$ [1900 units/mg, using the units of Lamy et al. (1980)]. Protein was estimated by the method of Bradford (1976), by using the Bio-Rad protein assay kit (Bio-Rad Laboratories GmbH), with bovine carbonic anhydrase (Sigma) as standard. The sample had an A_{413}/A_{280} ratio of 0.33 and a Mo/heme ratio of 0.56. Though it was not pure as judged by SDS gel electrophoresis, the EPR spectrum (Figure 5) was that specific for sulfite oxidase (Bray et al., 1983).

ENDOR Samples. For ENDOR work on xanthine oxidase, unless otherwise indicated, H1, H2 enzyme (Ventom et al., 1988) that was 50–60% functional was employed. Generation of different Mo(V) EPR signals was carried out generally as described in earlier work from this laboratory. In all cases, great care was taken to ensure that only a single Mo(V) EPR signal-giving species was present; 50 mM Na^+-Bicine buffer was used throughout. The Desulfo Inhibited signal was generated (Lowe et al., 1976) by treating the desulfo enzyme anaerobically with dithionite and ethylene glycol. Excess of these reagents was then removed by aerobic gel filtration, and the sample was concentrated. The formaldehyde Inhibited signal (Pick et al., 1971) was generated by treatment of the enzyme (0.4 mM) with 0.2 M formaldehyde for 2 h at approximately 25 °C, with continuous agitation in air. Excess formaldehyde was removed by gel filtration, and the sample was concentrated at 5 °C, by using a Minicon B-15 concentrator. The intensity of this signal begins to decrease 10–20 h after gel filtration (Morpeth & Bray, 1984), and the final concentration of the sample was rapidly achieved by blowing dry nitrogen over the surface of the stirred solution. The formamide Rapid signal (Morpeth et al., 1984) was generated by treating the enzyme (0.4 mM) with 0.4 M formamide for 40 min at approximately 25 °C and then concentrating aerobically at 5 °C, without removing excess substrate.

For sulfite oxidase, the low-pH chloride signal (Bray et al., 1983) was generated by reducing the enzyme aerobically, in 50 mM Na^+-PIPES buffer, pH 6.8, containing 0.1 M NaCl, for 1 min, with 10 mM Na_2SO_3.

ENDOR Measurements. ENDOR spectra were recorded on an updated Bruker ER 200D-SRC spectrometer equipped with an ENDOR/TRIPLE accessory and a radiofrequency amplifier of 100-W nominal output power (ENI 3100LA). Low-temperature measurements were made by using an Oxford Instruments ESR 900 cryostat modified to take sample tubes of up to 4-mm internal diameter. Recording conditions were generally as follows: temperature, 30 K; microwave power, 0.8 mW; radio-frequency power, 0-dB attenuation; modulation depth, 50 kHz; scan rate, 0.19 MHz s^{-1}. Any deviation from these conditions is noted in the figure legends. All ENDOR spectra illustrated were accumulated over extended periods, ranging from 2 to 18 h, to obtain adequate signal-to-noise ratios. To remove a number of features that were due to instrumental artifacts, a background spectrum, recorded under the same conditions as the experimental spectrum but at a magnetic field distant from the EPR spectrum, has in each case been digitally subtracted from the spectra illustrated. In Figures 2–5, EPR spectra of the samples used for ENDOR are illustrated. These were recorded at the same temperature as for the ENDOR, but at a microwave power of 0.1 mW.

Phosphorus Analysis. Samples were submitted to gel filtration (Sephadex G-25) and exhaustively dialyzed against 50 mM Na^+-Bicine buffer, pH 8.2, to remove traces of inorganic phosphate or pyrophosphate before analysis. Colorimetric

phosphorus analysis (Lowry et al., 1954) was performed after wet-ashing with perchloric and sulfuric acids (Hart et al., 1970), followed by pH adjustment with sodium acetate (Hasegawa et al., 1982).

NMR Spectra. ^{31}P NMR spectra were recorded on a Bruker WM-360 spectrometer at 145.7 MHz with a FT-pulse "flip angle" of 45°. To avoid localized heating of the sample, broad-band proton decoupling was not employed. Spectra from up to 90 000 acquisitions were accumulated over about 25 h. The viscosity of xanthine oxidase solutions (estimated by measuring the time for flow through a capillary) was found to increase rapidly upon raising the enzyme concentration above 1.4 mM, and the ^{31}P NMR spectrum of a 2.0 mM sample exhibited a complete lack of resolution. Accordingly, enzyme concentrations of 1.2–1.4 mM were generally employed. Spectra were recorded with the samples in 50 mM Na^+-Bicine buffer, pH 8.2, at 5 °C. The viscosity did not decrease greatly upon raising the temperature to 25 °C, and spectra at this temperature were not noticeably better resolved. Spectra obtained on a Bruker AMX-500 machine at 202.4 MHz were poorly resolved, presumably due to the field-dependent chemical shift anisotropy contribution to the relaxation rate of the ^{31}P nucleus (Vogel, 1984). The enzyme samples examined were of relatively low activity (30–60% functional) and did not contain any additions such as sodium salicylate.

Results and Discussion

Features in the ENDOR Spectra of Xanthine Oxidase Due to Coupling of ^{31}P to Molybdenum(V). As has been outlined in preliminary reports from this laboratory (Pinhal et al., 1989; Bray et al., 1991; Howes et al., 1990), features due to coupling of ^{31}P nuclei to molybdenum are observable in the ENDOR spectra of reduced xanthine oxidase samples that give rise to most if not all of the well-known (Bray, 1988; Bray & Gutteridge, 1982) molybdenum(V) EPR signals from this enzyme. These ENDOR features are centered on the ^{31}P Larmor frequency of about 5.9 MHz for a microwave frequency of 9.4 GHz and a g-value close to 2.

A typical ENDOR spectrum recorded over a relatively wide frequency range and centered on the phosphorus Larmor frequency is shown in Figure 1a. This spectrum was derived from a sample of xanthine oxidase giving the Desulfo Inhibited molybdenum(V) EPR signal, but basically similar features are present in all xanthine oxidase molybdenum(V) ENDOR spectra that we have examined. The doublet feature centered on 5.9 MHz clearly has a form that makes it a strong candidate to be ascribed to interaction with a single ^{31}P nucleus (or a number of such equivalent nuclei), with a coupling constant of about 0.2 MHz. There are, however, also features in the region of 7.0–7.6 MHz and at 4.5 MHz and below that might, as suggested in our preliminary work (Pinhal et al., 1989), be due to a phosphorus nucleus more strongly coupled to molybdenum (coupling constant about 3 MHz).

In order to identify conclusively which spectral features are due to phosphorus, we studied the variation of the ENDOR spectrum with microwave frequency. Figure 1a shows the ENDOR spectrum excited close to the g_2 EPR feature and recorded at 9.45 GHz, and Figure 1b shows the spectrum at the same point of the EPR spectrum but at 9.85 GHz. (Figure 1b was obtained by using a different microwave cavity mode from the one routinely used.) The magnetic fields used for Figure 1a,b were 342.48 and 356.35 mT, respectively. At the two fields, the ^{31}P Larmor frequencies, on which the ENDOR spectrum of this nucleus must be centered, are 5.91 and 6.15 MHz, respectively. The sharp doublet feature close to 6 MHz is shifted in Figure 1b relative to Figure 1a by exactly the

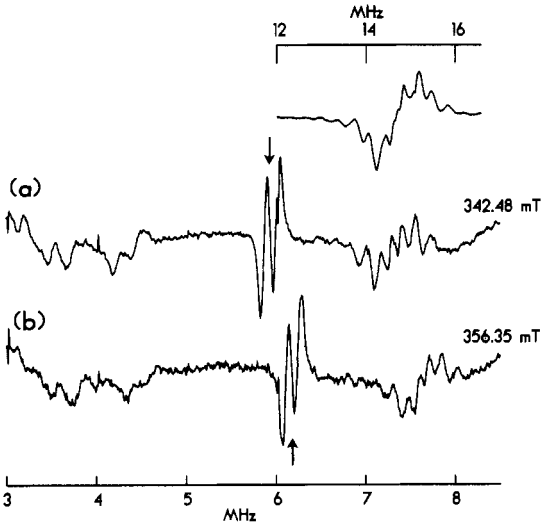

FIGURE 1: ENDOR spectra from the xanthine oxidase Desulfo Inhibited EPR signal stimulated near the g_2 position and recorded over a wide radio-frequency range. The magnetic field was 342.48 mT in (a) and 356.35 mT in (b). The arrows indicate the ^{31}P Larmor frequency for each spectrum. The scan rate was 0.33 MHz/s, the microwave power 0.65 mW, and the Mo(V) concentration 0.6 mM; other recording parameters were as listed under Experimental Procedures. The very sharp features apparent at 3.0, 4.0, and 6.0 MHz are instrumental artifacts. The inset spectrum at the top shows the ^{1}H ENDOR pattern corresponding to spectrum (a).

amount predicted (0.24 ± 0.01 MHz), which confirms that these lines are indeed due to ^{31}P. The features in the region of 7.3 MHz in Figure 1a, on the other hand, have shifted by 0.29 ± 0.02 MHz in Figure 1b and therefore are not part of a spectrum centered on the ^{31}P Larmor frequency and cannot be associated with this nucleus. These features are in fact symmetrical and centered on exactly half the ^{1}H Larmor frequency (7.29 or 7.59 MHz) in both Figure 1a and Figure 1b; taking this together with their strong similarity in shape to the true ^{1}H ENDOR spectrum (inset, Figure 1a), we assign these lines to a ^{1}H ENDOR spectrum excited by a second harmonic present in the radio-frequency signal supplied by our spectrometer. From the intensity of these signals relative to the true ^{1}H spectrum, we estimate that about 2% of the radio-frequency power is present in the second harmonic. This assignment is supported by our observation of features also centered at half the ^{1}H Larmor frequency in the ENDOR spectrum (not shown) of a frozen solution of $CuSO_4$. The features at 4.3 MHz and below are all shifted by less than 0.24 MHz in Figure 1b relative to Figure 1a, and thus cannot be due to ^{31}P. We are as yet unable to assign these low-frequency signals, though conceivably some features could be due to coupling to ^{23}Na nuclei (Larmor frequency, 3.859 MHz at 342.48 mT). It is clear, however, that only the lines in our spectra giving the doublet feature close to 6 MHz are due to ^{31}P.

Identity of the ^{31}P Nucleus Showing ENDOR Coupling to Molybdenum(V) in Xanthine Oxidase: Studies of the Deflavoenzyme. ENDOR spectra of the sharp doublet feature at 5.9 MHz, due to coupling to a single ^{31}P nucleus with a coupling constant of about 0.2 MHz, are illustrated for three molybdenum(V) xanthine oxidase species, Desulfo Inhibited, Inhibited, and Rapid, in Figures 2–4 and are considered in detail below. The xanthine oxidase half-molecule contains one phosphorus atom in its pterin molybdenum cofactor (Kramer et al., 1987), two more in its FAD (Bray, 1975), and, according to one report (Davis et al., 1984), another phosphorus as a phosphoserine residue. ENDOR spectroscopy can provide only limited data on the number of nonequivalent phosphate res-

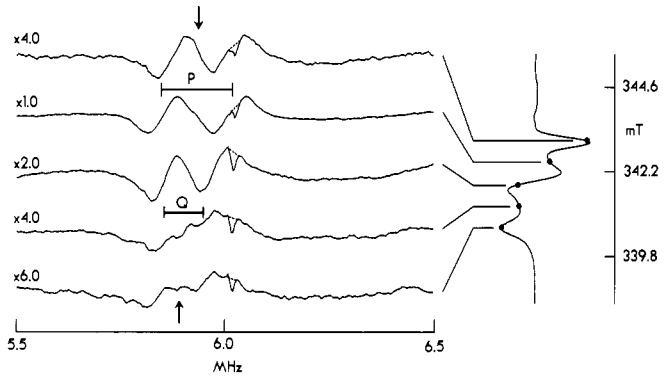

FIGURE 2: ENDOR spectra from the xanthine oxidase Desulfo Inhibited EPR signal recorded over a narrow radio-frequency range, at field settings as indicated on the right, across the entire EPR spectrum (the latter is shown with the magnetic field plotted vertically). The bar P gives a measure of $A_{\parallel}$, and bar Q is an upper limit for $A_{\perp}$. The arrows indicate the ^{31}P Larmor frequencies of the lowest and highest field ENDOR spectra. The microwave frequency was 9.45 GHz, and the microwave power and Mo(V) concentration were as Figure 1. The relative amplification of each spectrum is indicated. The sharp feature at approximately 6.0 MHz is an instrumental artifact, and a dashed line has been drawn to show the estimated effect of eliminating this.

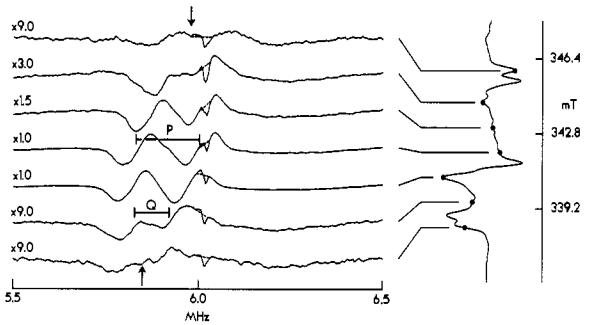

FIGURE 3: ENDOR spectra from the xanthine oxidase formaldehyde Inhibited EPR signal recorded at field settings across the EPR spectrum, as shown on the right. The bar P gives a measure of $A_{\parallel}$, and the bar Q is an upper limit for $A_{\perp}$. The arrows indicate the ^{31}P Larmor frequencies of the lowest and highest field ENDOR spectra. The microwave frequency was 9.45 GHz and the Mo(V) concentration 1.6 mM. The relative amplification of each spectrum is indicated. The sharp feature at approximately 6.0 MHz is an instrumental artifact, and a dashed line has been drawn to show the estimated effect of eliminating this.

idues present in the protein (those within ~10 Å from the molybdenum atom). Nevertheless, our first task was to attempt to determine which of the phosphorus atoms in the enzyme molecule was giving rise to the observed ^{31}P ENDOR spectra.

FAD may readily be removed (Bray, 1975) from xanthine oxidase, leaving the deflavoenzyme. We therefore compared the ^{31}P ENDOR spectra, for normal and deflavoenzyme samples, for the Desulfo Inhibited molybdenum(V) EPR signal. We could not distinguish the ENDOR of the deflavoenzyme from that of the normal form (Bray et al., 1991, and additional data not shown). This finding eliminates the two phosphorus atoms of the FAD molecule as the source of the coupled ^{31}P nuclei, leading us to conclude that these atoms must be at least 10 Å from molybdenum.

Evidence against Phosphoserine in the Xanthine Oxidase Molecule: Confirmation That ^{31}P of the Pterin Cofactor Is Coupled to Molybdenum. We next sought to confirm by colorimetric phosphorus analysis and by ^{31}P NMR the reported presence (Davis et al., 1984) of a phosphoserine residue in the xanthine oxidase molecule. As already noted, our preliminary results [reported in the proceedings of a symposium by Bray et al. (1991)] indicated this residue to be absent. As our work on this topic was completed, the publication of Johnson et al. (1989) provided clear evidence that phosphoserine is not present in the most highly purified xanthine oxidase samples. Our data confirming this conclusion are presented in brief outline below.

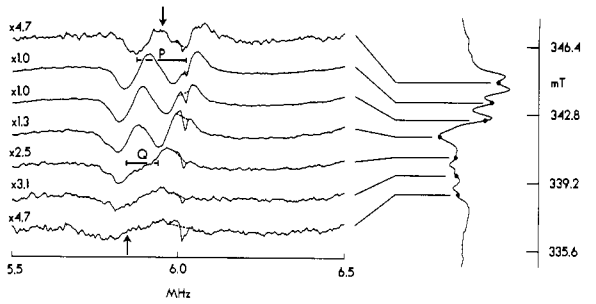

FIGURE 4: ENDOR spectra corresponding to the xanthine oxidase formamide Rapid type 1 EPR signal recorded at field settings across the EPR spectrum, as shown on the right. The bar P gives a measure of $A_{\parallel}$, and the bar Q is an upper limit for $A_{\perp}$. The arrows indicate the ^{31}P Larmor frequencies of the lowest and highest field ENDOR spectra. The microwave frequency was 9.47 GHz, the temperature 10 K, and the Mo(V) concentration 1.0 mM. The relative amplification of each spectrum is indicated. The sharp feature at approximately 6.0 MHz is an instrumental artifact, and a dashed line has been drawn to show the estimated effect of eliminating this.

Samples of xanthine oxidase prepared by the method of Hart et al. (1970) [procedure H1, H2 of Ventom et al. (1988)], having an A_{280}/A_{450} of about 6.0, were found to contain 5–6 mol of phosphorus/mol of enzyme, a high value that served to remind us of the high phosphoserine content of casein, a likely contaminant of incompletely purified milk xanthine oxidase samples. NMR examination revealed prominent peaks at about +3, −1, −9, and −14 ppm that are assigned [cf. Davis et al. (1984) and Johnson et al. (1989)], respectively, to phosphoserine, the pterin cofactor, and the two phosphorus atoms of FAD (these two resonances being rather broader than the other two). Additionally, our samples showed a sharp doublet centered on 11 ppm, which we ascribe to small amounts of free FAD (Kainosho & Kyoguku, 1972). More highly purified samples (as described under Experimental Procedures) gave an A_{280}/A_{450} ratio of 4.9 and contained 2.9–3.0 mol of phosphorus/mol of enzyme. NMR spectra were the same as those of the less purified samples, except that the phosphoserine[2] peak at +3 ppm was no longer detectable. Even more definitive, in view of a possible slight loss of flavin from the holoenzyme, was analysis of the deflavoenzyme (see Experimental Procedures) prepared from such a highly purified xanthine oxidase sample. This was found to contain 1.1 mol of phosphorus/mol of enzyme. The data are thus fully in accord with the conclusion of Johnson et al. (1989) that the xanthine oxidase molecule does not contain a phosphoserine residue.

As the phosphoserine is an impurity and the ^{31}P ENDOR is not due to FAD, then it is clear that it can only be due to phosphorus of the pterin molybdenum cofactor. Before proceeding on this assumption, however, we thought it prudent

[2] Davis et al. (1984) ascribed the peak they observed at +3 ppm on desulfo xanthine oxidase samples (i.e., 0% functional enzyme) to phosphoserine. They reported that the peak was of diminished intensity in samples that were 50–60% functional. Since our NMR samples were of rather low functionality, there should have been no problem in our detecting the proposed active-center phosphoserine had it been present. (Note that these workers have interchanged the signs of their chemical shift values in comparison with the more usual conventions that we have followed.)

Table I: ^{31}P Hyperfine Components and Mo to P Distances[a,b]

species	case 1					case 2				
	$A_\parallel$	$A_\perp$	A_{iso}	D	r (Å)	$A_\parallel$	$A_\perp$	A_{iso}	D	r (Å)
xanthine oxidase										
Desulfo Inhibited	0.17	−0.10	−0.010	0.090	7.1	0.17	0.10	0.125	0.025	11
Inhibited (formaldehyde)	0.17	−0.10	−0.010	0.090	7.1	0.17	0.10	0.125	0.025	11
Rapid type 1 (formamide)	0.15	−0.10	−0.015	0.085	7.3	0.15	0.10	0.115	0.015	12
sulfite oxidase										
low pH (chloride)	0.14	−0.10	−0.020	0.080	7.4	0.14	0.10	0.115	0.015	13

[a] Parameters were derived from the spectra in Figures 2–5. For definition, procedures, and explanations of case 1 and case 2, see the text. [b] Hyperfine coupling components and D are given in units of MHz.

to check that ^{31}P ENDOR spectra for xanthine oxidase preparations were not dependent on the purification procedure that was used. We therefore compared the ENDOR spectra of the Desulfo Inhibited species for two enzyme samples, prepared by the alternative procedures outlined above. Since as expected the spectra (data not shown) were indistinguishable from one another, we used the simpler H1, H2 purification procedure for all subsequent work, as described below.

Information on the Distance of Phosphorus of the Pterin Cofactor from Molybdenum. Information on the distance of the phosphorus atom from the paramagnetic molybdenum center is contained in the dipolar contribution to the anisotropic hyperfine interaction. In this case, the dipolar term is considered to be the dominant anisotropic contribution, as second-order exchange terms are expected to be small. The substantial **g** tensor anisotropy of the various xanthine oxidase species studied offers the opportunity to obtain ENDOR spectra with high orientation selectivity. This facilitates the determination of the dipolar hyperfine interaction by observing frozen solution ENDOR spectra as a function of the systematically changed field setting.

ENDOR spectra of the Desulfo Inhibited, formaldehyde Inhibited, and formamide Rapid type 1 signal-giving species of xanthine oxidase have been recorded for applied field settings across the entire envelope of $I = 0$ molybdenum(V) EPR features (Figures 2–4). As discussed above, the spectra are centered at approximately 5.9 MHz and are due to coupling to the phosphorus atom of the molybdenum cofactor. A set of equivalent phosphorus atoms gives rise to a pair of lines at $\nu = \nu_p \pm {}^1/_2A$, where ν_p is the ^{31}P Larmor frequency and A the hyperfine coupling constant. If the hyperfine interaction is isotropic, a single pair of peaks is seen whatever the field setting. However, anisotropy would split each of these lines into up to six components at g-values distant from the extremes in a low-symmetry environment (Hoffman et al., 1985). In this context, the observed variation in the line shape of the phosphorus features for all the species (Figures 2–4), as a function of field setting, is clearly related to the variations in the dipolar hyperfine coupling. As indicated above, such a series of spectra allows (Hughes et al., 1990) the extreme values of the hyperfine interaction to be extracted by observing the extremes of movement of the ENDOR lines in Figures 2–4. The extremes of movement correspond, for **A** axial, to the two principal hyperfine coupling components, $A_\parallel$ and $A_\perp$. (Note that, though the **g** tensor is rhombic the **A** tensor will be axial, since the anisotropic contribution is predominantly dipolar.)

If the phosphorus is not directly coordinated to the molybdenum, the main contributions to **A** will be an isotropic term, A_{iso}, and a dipolar term, A^D, which is given by

$$A^D = g_e\beta_e g_n\beta_n(3\cos^2\Phi - 1)/r^3$$

This equation assumes point dipolar interactions; r is the electron–nuclear distance and Φ the azimuthal angle away from the vector joining the center of electron spin density, assumed to be on the molybdenum, to the phosphorus. The extreme values of A^D are $A^D = 2D$ when $\Phi = 0°$ and $A^D = -D$ when $\Phi = 90°$, where $D = g_e\beta_e g_n\beta_n/r^3$. It follows that when $A_{iso} \neq 0$, the observed splittings are subject to the constraint $A_\parallel + 2A_\perp = 3A_{iso}$.

In the spectra of Figures 2–4, we have an experimental problem in determining accurately the extremes of movement, i.e., $A_\parallel$ and $A_\perp$. This is because the resolution of the spectra does not allow us to follow the position of the ^{31}P ENDOR lines at all field values. The maximum separation of the peaks, corresponding to $A_\parallel$, are clear and correspond to the lengths of the bars P in Figures 2–4. The values of the separation at their other turning points, corresponding to $A_\perp$, are difficult to estimate; they must, however, be less than the lengths of the bars Q in Figures 2–4. The length of bar Q corresponds to the hyperfine coupling (about 0.1 MHz) for which it is still just possible to resolve the two ^{31}P ENDOR peaks. The signs of $A_\perp$ in Figures 2–4 are obviously indeterminate since it is not possible to decide whether or not the lines have crossed through the ^{31}P Larmor frequency. We have therefore presented our results in Table I, allowing for both possibilities, by taking the extremes of the possible values of $A_\perp$ as minus and plus the lengths of the bars Q. The two limits for the range of D, and hence of r, are given in Table I. D is determined from the observed principal hyperfine components by using the relationship $A_\parallel - A_\perp = 3D$. In case 1, the sign of $A_\perp$ is taken as negative and in case 2 as positive; $A_\parallel$ is taken as positive in both cases. The molybdenum to phosphorus distance r can then be calculated from $(g_e\beta_e g_n\beta_n/D)^{1/3}$. Table I also shows the two limits for the range of A_{iso}. Comparison with the literature [e.g., see King (1976) and Schweiger (1982)] suggests that an isotropic coupling of 0.1 MHz over a distance of more than 7 Å is improbable. We therefore suggest that the true distances are likely to be nearer to the lower (case 1) rather than the upper (case 2) estimates of Table I, since the lower values require A_{iso} to be close to zero.

The molybdenum to cofactor phosphorus distances estimated (Table I) for the different xanthine oxidase species studied are seen to be quite similar to one another. The lower distance estimates are the same, within the experimental error of ±0.3 Å, at approximately 7.2 Å. Our distances may be compared with those expected on the basis of the cofactor structure as proposed by Rajagopalan and co-workers (Kramer et al., 1987; Johnson et al., 1990; Gruber et al., 1990). Model building on the basis of this structure indicates that, depending on the configuration of the pterin side chain, distances in the approximate range 2.5–8.5 Å would be expected, with, at the bottom end of this range, the possibility arising [cf. Künsthardt and Enemark (1987)] of the cofactor phosphate group becoming ligated to the molybdenum atom. Our preferred lower distance estimates are thus consistent with the evidence for the cofactor structure. We can therefore conclude that in all cases the conformation of the cofactor is an extended one, the possibility (Künsthardt & Enemark, 1987) than its phosphate

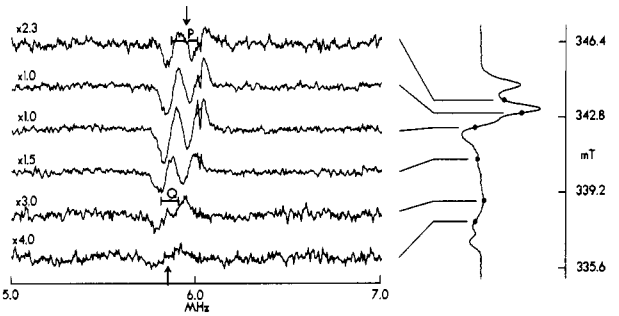

FIGURE 5: ENDOR spectra of the low-pH chloride EPR signal of sulfite oxidase recorded at field settings across the EPR spectrum, as shown on the right. (Note that the frequncy range illustrated is twice that in Figures 2–4.) The bar P gives a measure of $A_{\parallel}$, and bar Q is an upper limit for $A_{\perp}$. The arrows indicate the ^{31}P Larmor frequencies for the lowest and highest field ENDOR spectra. The microwave frequency was 9.46 GHz, microwave power 1.6 mW and the Mo(V) concentration 0.16 mM. The relative amplification of each spectrum is indicated. The sharp feature at approximately 6.0 MHz is an instrumental artifact, and a dashed line has been drawn to show the estimated effect of eliminating this.

group is ligated to the molybdenum being clearly excluded by our work.

The ^{31}P ENDOR spectra shown in Figure 5 are of the low-pH chloride species of chicken liver sulfite oxidase (Bray et al., 1983). The line shape bears a strong resemblance to the spectra, recorded under similar conditions, for xanthine oxidase (Figures 2–4). Because of the diluteness of the sample, spectra were recorded with signal-to-noise ratios worse than those for xanthine oxidase, and the width of the EPR spectrum was covered a little less fully. However, our estimate of the molybdenum to phosphorus distance for this species (Table I) is indeed close to the values obtained for xanthine oxidase. Sulfite oxidase contains phosphorus only in the form of a pterin cofactor molecule (Johnson et al., 1984) that is identical (Kramer et al., 1987) with that in xanthine oxidase. Our data therefore clearly indicate that the cofactor molecule in this enzyme is in an extended conformation, similar to that in xanthine oxidase.[3] This finding would appear to exclude the possibility of an altered cofactor conformation rather than different amino acid ligation to molybdenum [cf. Wootton et al. (1991)] providing the basis for the very different catalytic properties of sulfite oxidase compared to xanthine oxidase.

ACKNOWLEDGMENTS

We thank Dr. G. Lawless and Dr. A. Avent for carrying out the NMR measurements.

Registry No. Mo, 7439-98-7; P, 7723-14-0; xanthine oxidase, 9002-17-9; sulfite oxidase, 9029-38-3; molybdopterin, 89700-34-5; molybdoenzyme molybdenum cofactor, 73508-07-3.

REFERENCES

Bradford, M. (1976) *Anal. Biochem. 72*, 248–254.
Bray, R. C. (1975) *Enzymes (3rd Ed.) 12*, 299–419.
Bray, R. C. (1988) *Q. Rev. Biophys. 21*, 299–329.
Bray, R. C., & Gutteridge, S. (1982) *Biochemistry 21*, 5992–5999.
Bray, R. C., Gutteridge, S., Lamy, M. T., & Wilkinson, T. (1983) *Biochem. J. 211*, 227–236.
Bray, R. C., Howes, B. D., Bennett, B., & Lowe, D. J. (1991) in *Modern Trends in Biological Chemistry* (Ozawa, T., Ed.) Japan Scientific Societies Press, Tokyo (in press).
Davis, M. D., Edmondson, D. E., & Müller, F. (1984) *Eur. J. Biochem. 145*, 237–243.
Gruber, G., Kilpatrick, LaT., Bastian, N. R., Rajagopalan, K. V., & Spiro, T. G. (1990) *J. Am. Chem. Soc. 112*, 8179–8180.
Hart, L. I., McGartoll, M. A., Chapman, H. R., & Bray, R. C. (1970) *Biochem. J. 116*, 851–864.
Hasegawa, H., Parniak, M., & Kaufman, S. (1982) *Anal. Biochem. 120*, 360–364.
Hoffman, B. M., Venters, R. A., & Martinsen, J. (1985) *J. Magn. Reson. 62*, 537–542.
Howes, B. D., Pinhal, N. M., Turner, N. A., Bray, R. C., Anger, G., Ehrenberg, A., Raynor, J. B., & Lowe, D. J. (1990) *Biochemistry 29*, 6120–6127.
Howes, B. D., Bennett, B., Lowe, D. J., & Bray, R. C. (1991) in *Flavins and Flavoproteins* (Curti, B., et al., Eds.) DeGruyter, Berlin (in press).
Hughes, D. L., Lowe, D. J., Mohammed, M. Y., Pickett, C. J., & Pinhal, N. M. (1990) *J. Chem. Soc., Dalton Trans.*, 2021–2028.
Johnson, J. L., Hainline, B. L., Rajagopalan, K. V., & Arison, B. H. (1987) *J. Biol. Chem. 259*, 5414–5422.
Johnson, J. L., London, R. E., & Rajagopalan, K. V. (1989) *Proc. Natl. Acad. Sci. U.S.A. 86*, 6493–6497.
Johnson, J. L., Bastian, N. R., & Rajagopalan, K. V. (1990) *Proc. Natl. Acad. Sci. U.S.A. 87*, 3190–3194.
Kainosho, M., & Kyoguku, Y. (1972) *Biochemistry 11*, 741–752.
Kanda, M., & Rajagopalan, K. V. (1972) *J. Biol. Chem. 247*, 2177–2182.
Kessler, D. L., Johnson, J. L., Cohen, H. J., & Rajagopalan, K. V. (1974) *Biochim. Biophys. Acta 334*, 86–96.
King, F. W. (1976) *Chem. Rev. 76*, 157–186.
Komai, H., Massey, V., & Palmer, G. (1969) *J. Biol. Chem. 244*, 1692–1700.
Kramer, S. P., Johnson, J. L., Ribeiro, A., Millington, D. S., & Rajagopalan, K. V. (1987) *J. Biol. Chem. 262*, 16357–16363.
Künsthardt, V., & Enemark, J. H. (1987) *J. Chem. Soc. 109*, 7926–7927.
Lamy, M. T., Gutteridge, S., & Bray, R. C. (1980) *Biochem. J. 185*, 397–403.
Lowe, D. J., Barber, M. J., Pawlik, R. T., & Bray, R. C. (1976) *Biochem. J. 155*, 81–85.
Lowry, O. H., Roberts, N. R., Leiner, K. Y., Wu, M. L., & Farr, A. L. (1954) *J. Biol. Chem. 207*, 1–17.
Massey, V., & Edmondson, D. (1970) *J. Biol. Chem. 245*, 6595–6598.
Morpeth, F. F., & Bray, R. C. (1984) *Biochemistry 23*, 1332–1338.
Morpeth, F. F., George, G. N., & Bray, R. C. (1984) *Biochem. J. 220*, 235–242.
Nishino, T., Nishino, T., & Tsushima, K. (1981) *FEBS Lett. 131*, 369–372.
Pick, F. M., McGartoll, M. A., & Bray, R. C. (1971) *Eur. J. Biochem. 18*, 65–72.
Pinhal, N. M., Bray, R. C., Turner, N. A., & Lowe, D. J. (1989) in *Highlights of Modern Biochemistry*, (Kotyk, A., et al., Eds.) Vol. 1, pp 273–280, VSP, Zeist, The Netherlands.
Schweiger, A. (1982) *Struct. Bonding (Berlin) 51*, 1–128.

[3] The approximate orientation of the ^{31}P principal hyperfine component, $A_{\parallel}$ (corresponding to the Mo–P direction), with respect to the axes of the **g** tensor, can be seen to be the same (i.e., between g_2 and g_3 but nearer to g_2) for all three xanthine oxidase species (Figures 2–4) as well as for the low-pH chloride species of sulfite oxidase (Figure 5). This observation lends further support to the pterin cofactor having a similar orientation in the two enzymes.

Ventom, A. M., Deistung, J., & Bray, R. C. (1988) *Biochem. J. 255*, 949–956.
Vogel, H. J. (1984) in *Phosphorus-31 NMR: Principles and Applications* (Gorenstein, D. G., Ed.) pp 105–154, Academic Press, New York.
Wootton, J. C., Nicolson, R. E., Cock, J. R., Walters, D. E., Burke, J., Doyle, W., & Bray, R. C. (1991) *Biochim. Biophys. Acta* (in press).

Ligand Binding and Protein Relaxation in Heme Proteins: A Room Temperature Analysis of NO Geminate Recombination†

J. W. Petrich,‡,§ J.-C. Lambry,‡ K. Kuczera,∥ M. Karplus,*,∥ C. Poyart,⊥ and J.-L. Martin*,‡
Laboratoire d'Optique Appliquée, Ecole Polytechnique, ENSTA, INSERM U275, 91128 Palaiseau Cedex, France, Department of Chemistry, Harvard University, Cambridge, Massachusetts 02138, and INSERM U299, 94275 Le Kremlin-Bicêtre, France
Received July 10, 1990; Revised Manuscript Received November 1, 1990

ABSTRACT: Ultrafast absorption spectroscopy is used to study heme–NO recombination at room temperature in aqueous buffer on time scales where the ligand cannot leave its cage environment. While a single barrier is observed for the cage recombination of NO with heme in the absence of globin, recombination in hemoglobin and myoglobin is nonexponential. Examination of hemoglobin with and without inositol hexaphosphate points to proximal constraints as important determinants of the geminate rebinding kinetics. Molecular dynamics simulations of myoglobin and heme–imidazole subsequent to ligand dissociation were used to investigate the transient behavior of the Fe–proximal histidine coordinate and its possible involvement in geminate recombination. The calculations, in the context of the absorption measurements, are used to formulate a distinction between nonexponential rebinding that results from multiple protein conformations (substates) present at equilibrium or from nonequilibrium relaxation of the protein triggered by a perturbation such as ligand dissociation. The importance of these two processes is expected to depend on the time scale of rebinding relative to equilibrium fluctuations and nonequilibrium relaxation. Since NO rebinding occurs on the picosecond time scale of the calculated myoglobin relaxation, a time-dependent barrier is likely to be an important factor in the observed nonexponential kinetics. The general implications of the present results for ligand binding in heme proteins and its time and temperature dependence are discussed. It appears likely that, at low temperatures, inhomogeneous protein populations play an important role and that as the temperature is raised, relaxation effects become significant as well.

The microscopic aspects of ligand binding in myoglobin and hemoglobin are not fully understood, although great progress has been made recently in their analysis. Structural disorder and its temporal evolution (Frauenfelder et al., 1979; Case & Karplus, 1979; Debrunner & Frauenfelder, 1982; Elber & Karplus, 1987a,b) apparently play an important role. The high-resolution X-ray structures of ligated and unligated myoglobin do not reveal any path by which ligands can move between the heme binding site and the outside of the protein (Perutz & Mathews, 1966; Takano, 1977). Since motion must therefore be involved in the ligand binding, myoglobin has become a model system for studying the relation of motion to function in proteins.

Much of what is known about the influence of protein fluctuations on heme protein reactivity is due to measurements of ligand recombination after photodissociation on the nanosecond to second time scales. A series of studies (Austin et al., 1975; Henry et al., 1983; Ansari et al., 1985) have suggested that a phenomenological description of the kinetics of photodissociation and rebinding of a ligand X to myoglobin (Mb) can be written as

$$\mathrm{MbX} \rightleftarrows (\mathrm{Mb} + \mathrm{X})_{\mathrm{pocket}} \rightleftarrows (\mathrm{MB} + \mathrm{X})_{\mathrm{protein}} \rightleftarrows (\mathrm{Mb} + \mathrm{X})_{\mathrm{solution}}$$

where the subscript refers to the location of the ligand X. Each of the designated species may involve several different states or substates on a microscopic level. At low temperatures (below 200 K in ethylene glycol/water), it is found that the geminate rebinding of the CO ligand is nonexponential. This has been attributed to a distribution of barrier heights, associated with the different substates that equilibrate slowly relative to the rebinding. As the temperature is raised, the geminate recombination of CO becomes exponential and can be described by a single barrier.

In analyzing the origin of the nonexponential behavior and, more generally, the complexity of the rebinding kinetics in proteins, it is important to consider two types of motional phenomena (Ansari et al., 1985). One of these consists of the fluctuations that occur at equilibrium. These equilibrium fluctuations consist of motions within a potential well at low temperature. At higher temperatures transitions between wells are superposed on the harmonic fluctuations (Elber & Karplus, 1987; Smith et al., 1990). The other type of motion arises in a nonequilibrium system and corresponds to relaxation toward equilibrium. Since photodissociation creates a nonequilibrium

† During the course of this work, J.W.P. was the recipient of an NSF Industrialized Countries postdoctoral fellowship, an INSERM *poste orange*, and fellowships from La Fondation pour la Recherche Médicale and the Ecole Polytechnique. Parts of this work were funded by INSERM, ENSTA, le Ministre de la Recherche et de la Technologie, the National Science Foundation, and the National Institutes of Health.
‡ INSERM U275.
§ Present address: Department of Chemistry, Iowa State University, Ames, IA 50011.
∥ Harvard University.
⊥ INSERM U299.

0006-2960/91/0430-3975$02.50/0